

# The Versatile 2-Substituted Imidazoline Nucleus as a Structural Motif of Ligands Directed to the Serotonin 5-HT<sub>1A</sub> Receptor

Fabio Del Bello,<sup>[a]</sup> Antonio Cilia,<sup>[b]</sup> Antonio Carrieri,<sup>[c]</sup> Domenico Claudio Fasano,<sup>[c]</sup> Carla Ghelardini,<sup>[d]</sup> Lorenzo Di Cesare Mannelli,<sup>[d]</sup> Laura Micheli,<sup>[d]</sup> Carlo Santini,<sup>[e]</sup> Eleonora Diamanti,<sup>[a]</sup> Mario Giannella,<sup>\*,[a]</sup> Gianfabio Giorgioni,<sup>[a]</sup> Valerio Mammoli,<sup>[a]</sup> Corinne Dalila Paoletti,<sup>[a]</sup> Riccardo Petrelli,<sup>[a]</sup> Alessandro Piergentili,<sup>[a]</sup> Wilma Quaglia,<sup>[a]</sup> and Maria Pigni<sup>[a]</sup>

Dedicated to Prof. Maria Pigni, who passed away on February 8, 2016.

The involvement of the serotonin 5-HT<sub>1A</sub> receptor (5-HT<sub>1A</sub>-R) in the antidepressant effect of allyphenylene and its analogues indicates that ligands bearing the 2-substituted imidazoline nucleus as a structural motif interact with 5-HT<sub>1A</sub>-R. Therefore, we examined the 5-HT<sub>1A</sub>-R profile of several imidazoline molecules endowed with a common scaffold consisting of an aromatic moiety linked to the 2-position of an imidazoline nucleus by a biatomic bridge. Our aim was to discover other ligands targeting 5-HT<sub>1A</sub>-R and to identify the structural features favoring 5-HT<sub>1A</sub>-R interaction. Structure–activity relationships, supported

by modeling studies, suggested that some structural cliché such as a polar function and a methyl group in the bridge, as well as proper steric hindrance in the aromatic area of the above scaffold, favored 5-HT<sub>1A</sub>-R recognition and activation. We also highlighted the potent antidepressant-like effect (mouse forced swimming test) of (S)-(+)-**19** [(S)-(+)-naphthyl] at very low dose (0.01 mg kg<sup>-1</sup>). This effect was clearly mediated by 5-HT<sub>1A</sub> as it was significantly reduced by pretreatment with the 5-HT<sub>1A</sub> antagonist WAY100635.

## Introduction

The 2-substituted imidazoline ring is a well-known, versatile structural motif that is present in various ligands interacting with different biological targets. Many pharmacological applications of imidazoline compounds in therapeutic areas such as cardiovascular, metabolic, and psychiatric disorders can be ascribed to modulation of  $\alpha$ -adrenergic receptors ( $\alpha$ -ARs) and/or the imidazoline binding sites (IBS), as reported in a number of excellent reviews.<sup>[1,2]</sup> Moreover, there is a wealth of data about

the biological activity of 2-imidazolines that is extended far beyond their traditional targets (i.e.,  $\alpha$ -ARs/IBS), which supports the privileged character of the 2-imidazoline nucleus.<sup>[3]</sup>

For several years, our studies have focused on the design and preparation of active ligands directed to different biological systems and characterized by common scaffold **I** reported in Figure 1 containing the imidazoline nucleus as a basic function. Our experience also highlighted that the bridge (X) and the aromatic area (Ar) forming the substituent in the 2-position of the imidazoline nucleus display different functions. Indeed,

[a] Dr. F. Del Bello, Dr. E. Diamanti, Prof. M. Giannella, Dr. G. Giorgioni, Dr. V. Mammoli, C. D. Paoletti, Dr. R. Petrelli, Prof. A. Piergentili, Prof. W. Quaglia, Prof. M. Pigni  
School of Pharmacy, Medicinal Chemistry Unit, University of Camerino, Via S. Agostino 1, 62032 Camerino (Italy)  
E-mail: mario.giannella@unicam.it

[b] Dr. A. Cilia  
Recordati S.p.A., Drug Discovery, via Civitali 1, 20148 Milano (Italy)

[c] Prof. A. Carrieri, D. C. Fasano  
Department of Pharmacy-Drug Science, University of Bari "Aldo Moro", Via E. Orabona 4, 70125 Bari (Italy)

[d] Prof. C. Ghelardini, Dr. L. Di Cesare Mannelli, L. Micheli  
Department of Neuroscience, Psychology, Drug Research and Child Health - Neurofarba - Pharmacology and Toxicology Section, University of Florence, Viale Pieraccini 6, 50039 Firenze (Italy)

[e] Prof. C. Santini  
School of Science and Technology, University of Camerino, Via S. Agostino 1, 62032 Camerino (Italy)

Supporting Information for this article can be found under <http://dx.doi.org/10.1002/cmdc.201600383>.

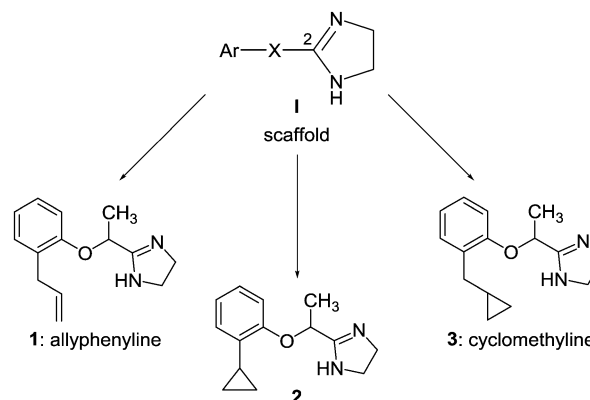
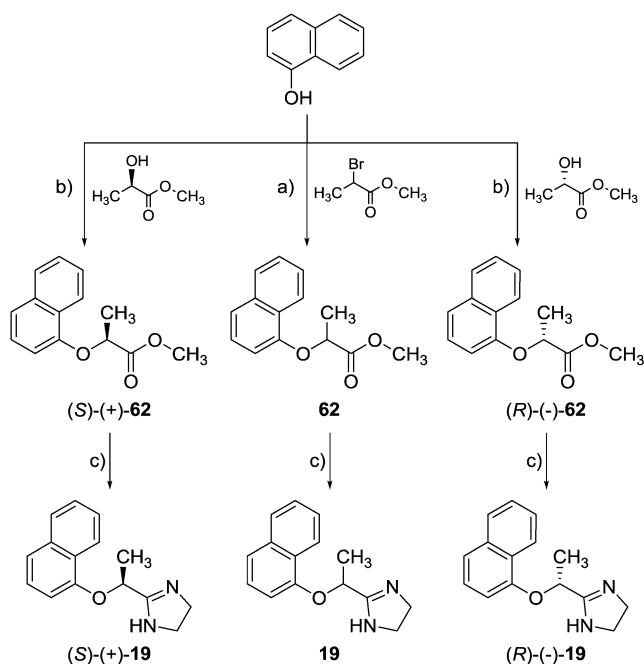


Figure 1. Biologically active ligands 1–3 sharing a common scaffold **I**.





**Scheme 1.** Reagents and conditions: a)  $K_2CO_3$ , 1,2-dimethoxyethane (DME), reflux, 18 h; b) diisopropyl azodicarboxylate (DIAD),  $Ph_3P$ , THF, RT, 20 h; c)  $NH_2CH_2CH_2NH_2$ ,  $Al(CH_3)_3$ , toluene, 65 °C, 5 h.

(-)-2-(Naphthalen-1-yloxy)propanoic acid methyl ester [(S)-(+)-**62** and (R)-(-)-**62**, respectively] were obtained by Mitsunobu reaction by using commercially available naphthalen-1-ol and methyl (R)-(-)- or (S)-(+)-lactate, respectively, with inversion of configuration.<sup>[29]</sup> The reaction of racemic **62**, (S)-(+)-**62**, or (R)-(-)-**62** with ethylenediamine in the presence of  $Al(CH_3)_3$  yielded corresponding imidazoline **19**, (S)-(+)-**19**, or (R)-(-)-**19**, respectively.

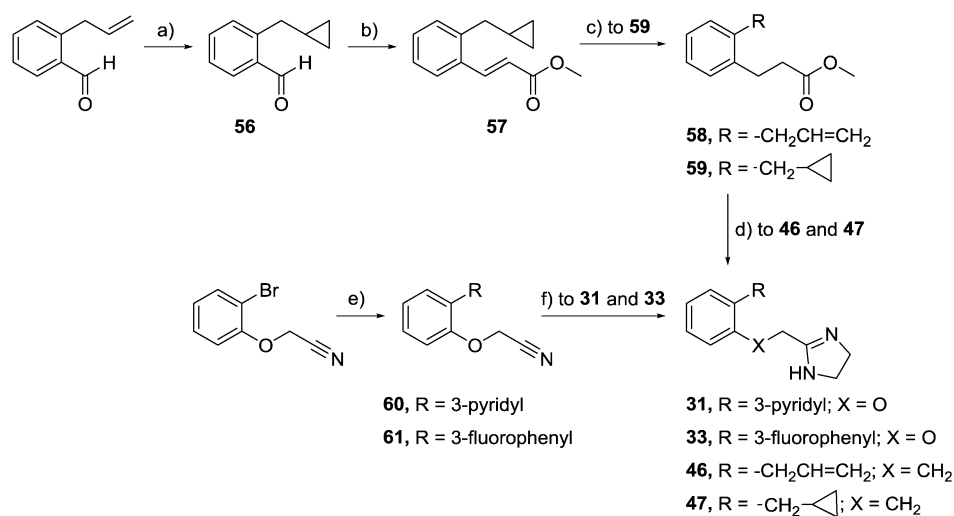
The enantiomeric excess (*ee*), determined by  $^1H$  NMR spectroscopy, was approximately 85%, owing to partial racemiza-

tion under the reaction conditions. Indeed, the spectra of enantiomers and racemic **19** upon the addition of (S)-(+)-2,2,2-trifluoro-1-(9-anthryl)ethanol as a chiral shift reagent showed a doublet of doublets at  $\delta = 1.56$  ppm for the methyl protons. Therefore, imidazoline **19** was resolved into (S)-(+)-**19** and (R)-(-)-**19** by fractional crystallization of the (+)-di-*O,O'*-dibenzoyl-D-tartrate and (-)-di-*O,O'*-dibenzoyl-L-tartrate salts, respectively. Their *ee* values, determined by  $^1H$  NMR spectroscopy, were found to be >98% for both enantiomers. In this case, the  $^1H$  NMR spectra, similarly performed, for the methyl group of (S)-(+)-**19** and (R)-(-)-**19** only showed one doublet at  $\delta = 1.59$  and 1.53 ppm, respectively.

Imidazolines **31**, **33**, **46**, and **47** were prepared according to the synthetic procedure reported in Scheme 2. The reaction of 2-allylbenzaldehyde with  $Et_2Zn$  and  $CH_2I_2$  gave intermediate **56**, the treatment of which with methyl 2-(diethoxyphosphoryl)acetate in the presence of NaH afforded **57**. Subsequent catalytic hydrogenation by using 10% Pd/C as the catalyst yielded ester **59**. The condensation of **58**<sup>[30]</sup> and **59** with ethylenediamine in the presence of  $Al(CH_3)_3$  afforded imidazolines **46** and **47**, respectively. The reactions of 2-(2-bromophenoxy)acetonitrile<sup>[31]</sup> with 3-pyridylboronic acid and 3-fluorophenylboronic acid in the presence of tetrakis(triphenylphosphine)palladium(0) gave nitriles **60** and **61**, respectively, which were condensed with ethylenediamine to obtain corresponding imidazolines **31** and **33**.

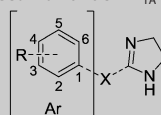
### SAR study

The 5-HT<sub>1A</sub>-R affinity values (*pK<sub>i</sub>*) of all compounds are reported in Tables 1 and 2 along with the agonist potency (*pD<sub>2</sub>*) and relative efficacy (%*E<sub>max</sub>*) of some of them. They were determined on HeLa cells expressing human cloned 5-HT<sub>1A</sub>-R, according to previously described procedures.<sup>[32]</sup> The 5-HT<sub>1A</sub> agonist 8-hydroxy-2-(di-*n*-propylamino)tetraline (8-OH-DPAT) was included as a standard compound.



**Scheme 2.** Reagents and conditions: a)  $Et_2Zn$ ,  $CH_2I_2$ ,  $CF_3CO_2H$ , RT, 2 h; b) methyl 2-(diethoxyphosphoryl)acetate, NaH, THF, RT, 3 h; c)  $H_2$  (0.34 MPa), 10% Pd/C,  $CH_3OH$ , RT, 20 h; d)  $NH_2CH_2CH_2NH_2$ ,  $Al(CH_3)_3$ , toluene, reflux, 20 h; e) 3-pyridylboronic acid for **60**, 3-fluorophenylboronic acid for **61**,  $Pd[(C_6H_5)_3P]_4$ , 1 N  $Na_2CO_3$ , DME, reflux, 20 h; f)  $NH_2CH_2CH_2NH_2$ , reflux, 20 h.

**Table 1.** Affinity constants ( $pK_i$ ), agonist efficacies ( $pD_2$ ), and relative efficacies ( $\% E_{\max}$ ) on human recombinant 5-HT<sub>1A</sub>-R.



Compound	R	MR <sup>[a]</sup>	X	$pK_i$ <sup>[b]</sup>	$pD_2$ <sup>[c]</sup>	$\% E_{\max}$ <sup>[d]</sup>
<b>1</b> <sup>[7]</sup> allyphenylene	2,	14.75		7.55	6.86	67
(S)-(+)- <b>1</b> <sup>[9]</sup>	2,	14.75		7.45	7.19	96
(R)-(-)- <b>1</b> <sup>[9]</sup>	2,	14.75		< 6	-	-
<b>2</b> <sup>[8]</sup>	2,	12.85		8.03	7.24	92
(S)-(+)- <b>2</b> <sup>[9]</sup>	2,	12.85		8.22	7.86	102
(R)-(-)- <b>2</b> <sup>[9]</sup>	2,	12.85		< 6	-	-
<b>3</b> <sup>[10]</sup> cyclopropylmethyl	2,	17.45		7.98	7.20	75
(S)-(+)- <b>3</b> <sup>[11]</sup>	2,	17.45		8.24	7.40	97
(R)-(-)- <b>3</b> <sup>[11]</sup>	2,	17.45		7.40	6.80	68
<b>4</b> <sup>[22]</sup>	H	-		< 6	-	-
<b>5</b> <sup>[8]</sup>	2, H <sub>3</sub> C	5.50		< 6	-	-
<b>6</b> <sup>[10]</sup>	2,	6.22		< 6	-	-
<b>7</b> <sup>[10]</sup>	2, H <sub>3</sub> CO	7.51		< 6	-	-
<b>8</b> <sup>[10]</sup>	2,	10.69		< 6	-	-
<b>9</b> <sup>[10]</sup>	2,	14.72		7.72	7.04	121.1
<b>10</b> <sup>[8]</sup>	2,	14.71		7.86	7.08	118
<b>11</b> <sup>[7]</sup>	2,	22.05		8.16	-	-
<b>12</b> <sup>[6]</sup>	2,	22.99		6.82	-	-
<b>13</b> <sup>[6]</sup>	2,	23.44		7.10	6.58	79.34
<b>14</b> <sup>[6]</sup>	2,	23.44		6.88	-	-
<b>15</b> <sup>[6]</sup>	2,	22.71		7.67	-	-
(S)-(+)- <b>15</b> <sup>[9]</sup>	2,	22.71		7.73	-	-
(R)-(-)- <b>15</b> <sup>[9]</sup>	2,	22.71		7.41	-	-
<b>16</b> <sup>[22]</sup> biphenylene	2,	25.60		7.34	6.3	120.2
(S)-(-)- <b>16</b> <sup>[22]</sup>	2,	25.60		7.60	-	-
(R)-(+)- <b>16</b> <sup>[22]</sup>	2,	25.60		6.60	-	-

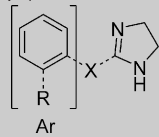
**Table 1.** (Continued)

Compound	R	MR <sup>[a]</sup>	X	$pK_i$ <sup>[b]</sup>	$pD_2$ <sup>[c]</sup>	$\% E_{\max}$ <sup>[d]</sup>
<b>17</b> <sup>[22]</sup>	3,	25.60		< 6	-	-
<b>18</b> <sup>[22]</sup>	4,	25.60		< 6	-	-
<b>19</b>	2,3,	17.37		8.13	7.31	111.8
(S)-(+)- <b>19</b>	2,3,	17.37		8.89	-	-
(R)-(-)- <b>19</b>	2,3,	17.37		7.14	-	-
<b>20</b> <sup>[24]</sup>	3,4,	17.37		< 6	-	-
<b>21</b> <sup>[6]</sup>	2,	25.82		7.60	6.85	79.55
<b>22</b> <sup>[6]</sup> <i>m</i> -nitrobiphenylene	2,	31.92		7.74	-	-
(S)-(-)- <b>22</b> <sup>[26]</sup>	2,	31.92		7.95	-	-
(R)-(+)- <b>22</b> <sup>[26]</sup>	2,	31.92		7.02	-	-
<b>23</b> <sup>[7]</sup>	2,	25.65		8.25	-	-
<b>24</b> <sup>[22]</sup>	H	-		< 6	-	-
<b>25</b> <sup>[8]</sup>	2, H <sub>3</sub> C	5.50		< 6	-	-
<b>26</b> <sup>[8]</sup> cirazoline	2,	12.85		7.46	-	-
<b>27</b> <sup>[5]</sup>	2,	14.72		7.56	6.67	102.3
<b>28</b> <sup>[8]</sup>	2,	14.71		7.12	-	-
<b>29</b> <sup>[5]</sup>	2,	14.75		7.15	-	-
<b>30</b> <sup>[5]</sup>	2,	17.45		7.18	6.25	118.9
<b>31</b>	2,	23.44		6.60	-	-
<b>32</b> <sup>[22]</sup>	2,	25.60		6.63	5.35	103.2
<b>33</b>	2,	25.82		6.53	-	-
<b>34</b> <sup>[22]</sup>	2,	25.60		7.20	6.80	80
<b>35</b> <sup>[24]</sup>	H	-		< 6	-	-
<b>36</b> <sup>[22]</sup>	2,	25.60		6.62	5.5	150.4
8-OH-DPAT				8.47	-	-

[a] MR of substituent R calculated according to Viswanadhan et al.<sup>[33]</sup>

[b] Affinity estimates were derived from the displacement of [<sup>3</sup>H]8-hydroxy-2-(di-*n*-propylamino)tetralin binding for 5-HT<sub>1A</sub> receptor. Each experiment was performed in triplicate.  $K_i$  values were from two to three experiments, which agreed within  $\pm 20\%$ . [c]  $pD_2$  values are the negative logarithm of the agonist concentration required to obtain 50% of the maximal stimulation of [<sup>35</sup>S]GTP $\gamma$ S binding and were calculated from two to three experiments, which agreed within  $\pm 20\%$ . [d] Maximal stimulation is expressed as a percentage of the maximal 5-HT response.

**Table 2.** Affinity constants ( $pK_i$ ) on human recombinant 5-HT<sub>1A</sub>-R.



Compound	R	MR <sup>[a]</sup>	X	$pK_i$ <sup>[b]</sup>
37 <sup>[4]</sup>	H <sup>----</sup>	–		< 6
38 <sup>[20]</sup> carbomethylene	H <sub>3</sub> C <sup>----</sup>	5.50		< 6
39 <sup>[20]</sup>	Cl <sup>----</sup>	5.81		< 6
40 <sup>[20]</sup>		23.44		< 6
41 <sup>[20]</sup>		22.71		< 6
42 <sup>[20]</sup>		25.60		< 6
43 <sup>[20]</sup>		27.58		< 6
44 <sup>[21]</sup> phenyzoline	H <sup>----</sup>	–		< 6
45 <sup>[23]</sup>	Cl <sup>----</sup>	5.81		< 6
46		14.75		< 6
47		17.45		< 6
48 <sup>[23]</sup>		22.71		< 6
49 <sup>[23]</sup>		25.60		< 6
50 <sup>[23]</sup>		31.92		< 6
51 <sup>[24]</sup>	H <sup>----</sup>	–		< 6
52 <sup>[25]</sup>	H <sub>3</sub> C <sup>----</sup>	5.50		< 6
53 <sup>[25]</sup>	Cl <sup>----</sup>	5.81		< 6
54 <sup>[25]</sup>	H <sub>3</sub> CO <sup>----</sup>	7.51		< 6
55 <sup>[25]</sup>	O <sub>2</sub> N <sup>----</sup>	6.08		< 6
8-OH-DPAT				8.47

[a] MR of substituent R calculated according to Viswanadhan et al.<sup>[33]</sup>  
 [b] Affinity estimates were derived from the displacement of [<sup>3</sup>H]8-hydroxy-2-(di-*n*-propylamino)tetralin binding for 5-HT<sub>1A</sub> receptor. Each experiment was performed in triplicate.  $K_i$  values were from two to three experiments, which agreed within  $\pm 20\%$ .

Analysis of the results showed that 5-HT<sub>1A</sub>-R interaction was strongly affected by the chemical features of the bridge. Indeed, as observed in Table 2, a wholly carbon bridge provided ligands devoid of significant affinity ( $pK_i < 6$ ). In contrast, the presence of polar functions such as an oxygen atom or an NH group in the bridge favored the 5-HT<sub>1A</sub>-R recognition, as highlighted by the good affinity shown by most of the compounds reported in Table 1.

The functional study revealed that the affinity was also associated with the ability of the ligand to activate 5-HT<sub>1A</sub>-R. Indeed, in addition to what was reported for 1–3, imidazolines 9, 10, 13, 16, 19, 21, 27, 30, 32, 34, and 36 behaved as 5-HT<sub>1A</sub>

agonists. Interestingly, our study allowed additional observations useful for the building of ligands directed to 5-HT<sub>1A</sub>-R. Indeed, the observation that the affinities of 1, 2, 3, 9, 10, 13, 16, 21, and 34, all bearing a methyl group in the bridge, were higher than those of their desmethyl analogues 29, 26, 30, 27, 28, 31, 32, 33, and 36, respectively, highlighted the advantageous role played by this group. The weak affinity displayed by unsubstituted derivatives 4, 24, and 35 indicated that 5-HT<sub>1A</sub>-R recognition was also affected by the presence of decorations inserted in the aromatic region. In addition, substitution in the *ortho* position proved to be determinant, as indicated by the lack of affinity of the *meta* (see compound 17) and *para* (see compound 18) regioisomers of 16. A behavior similar to that of the *ortho*-phenyl-substituted derivatives was displayed by 19, which can be considered the constrained analogue of 16. Indeed, it showed high 5-HT<sub>1A</sub>-R affinity and efficacious agonist potency similar to that of 8-OH-DPAT. In contrast,  $\beta$ -naphthyl isomer 20, the constrained analogue of *para*-substituted derivative 18, displayed a negligible 5-HT<sub>1A</sub>-R profile. Among the peculiar characteristics of the *ortho* substituent, the steric hindrance (MR)<sup>[33]</sup> played an important role. Indeed, groups with MR values from 12.85 to 31.92 induced a significant 5-HT<sub>1A</sub>-R interaction, whereas those with minor steric hindrance (MR values from 5.50 to 10.69) proved to be unsuitable. Anyway, aliphatic and aromatic substituents were similarly accepted. On the other hand, a reduced aromaticity of the *ortho*-phenyl substituent owing to the presence of polar functions did not significantly affect the 5-HT<sub>1A</sub>-R interaction (cf. 16 with 12–14, 21, and 22). This observation was supported by the comparison of desmethyl derivative 32 with its analogues 31 and 33. Noteworthy, suitable aromatic and aliphatic *ortho* substituents had a favorable role only in the presence of a proper bridge, as suggested by the lack of affinity shown by 40–42 and 46–50, all bearing a wholly carbon bridge.

Interestingly, the size of the substituent also appeared to govern the behavior of the chiral compounds. Indeed, though all the *S* enantiomers showed affinities higher than those of the *R* enantiomers, only in the case of the derivatives bearing an *ortho* substituent of suitable size did both enantiomers possess significant 5-HT<sub>1A</sub>-R affinity (cf. the enantiomers of 3, 15, 16, and 22 with those of 1 and 2).

### Molecular modeling

Within this large pavilion of chemical and structural observations, the aforementioned instances were interpreted *in silico*, and the results were in agreement with the *in vitro* data. In fact, by means of a 5-HT<sub>1A</sub>-R homology model obtained by using the recently resolved structure of the human serotonin 5-HT<sub>1B</sub>-R in complex with the serotonergic agonist ergotamine (PDB ID: 4IAR),<sup>[34]</sup> molecular dynamics (MD) simulations were performed on selected enantiomers 1 and 19. This choice was guided by the insight gained from the SAR study: indeed the affinity of (*S*)-(+)-19 was almost two orders of magnitude higher than that of (*R*)-(–)-19 and that of (*S*)-(+)-1, which suggested the pivotal role of the stereochemistry and the need of a bulky substituent. Derivative (*R*)-(–)-1 with the

lowest  $pK_i$ , lacking the aforementioned critical features, served us at the three-dimensional level as a negative control.

Our main goal was initially to prove stronger stability for the (S)-(+)-**19**/5-HT<sub>1A</sub>-R complex with respect to the (R)-(-)-**1**/5-HT<sub>1A</sub>-R complex and then to address four significant issues relating structural and chemical properties to affinity: one, the merit of the charged imidazoline nucleus in receptor binding; two, the size of the *ortho* substituent; three, the role of the proper configuration of the asymmetric carbon atom; four, the need of a polar function in the bridge. For the examined binders, reliable binding modes, as well as consistent ligand interaction patterns also in agreement with site-directed mutagenesis (SDM) data, were indeed achieved.

First of all, it was observed that all the studied receptor–ligand complexes showed strong stability within the typical G-protein-coupled receptor  $\alpha$ -helix motif, as suggested by low ( $<2.5$  Å) fluctuations for the residues spanning the transmembrane domain measured along the trajectories (see Figure 3).

In contrast, the strongest difference might be observed within the region including the second extracellular loop (i.e., residues 179–191), at which the largest oscillation of the C $\alpha$  trace atoms is observed only in low-affinity derivative (R)-(-)-**1**, which suggests that in this receptor moiety, critical contacts, most likely affected by stereochemistry, should take place. Moreover from the data reported in Table 3, it is worth noting that more favorable interaction energies are scored relative to compounds having similar chirality but carrying a different substituent: indeed, both enantiomers of **19** showed better mean values with respect to the enantiomers of **1**. These data supported our first hypothesis advising a large and more hindered substituent over a smaller one for high-affinity binders

**Table 3.** Mean interaction energy (MIE) and C $\alpha$  atom displacement (RMSF) measured along the molecular dynamics runs.

Compd	MIE [kJ mol <sup>-1</sup> ]	RMSF
(R)-(-)- <b>1</b>	$-203.56 \pm 17.30$	$2.31 \pm 1.64$
(S)-(+)- <b>1</b>	$-175.55 \pm 23.34$	$2.06 \pm 1.28$
(R)-(-)- <b>19</b>	$-215.13 \pm 16.80$	$2.59 \pm 1.87$
(S)-(+)- <b>19</b>	$-229.25 \pm 8.00$	$2.13 \pm 1.62$

and also proved that for imidazoline **19** the S configuration was better than the R configuration.

MD also highlighted the binding feature of our ligands: as in the majority of serotonergic receptor–(ant)agonist complexes, our binders are accommodated in a quite wide and accessible cleft defined within the upper part of the third, sixth, and seventh transmembrane helices, and moreover, time-line analysis of the protein–ligand interactions pattern detected some critical hot spots most likely characterizing the receptor cavity. As it might be perceived from Figure 4 depicting the frequency of positive contacts between the ligands and the binding site residues, the basic imidazoline ring is engaged through a charged reinforced hydrogen bond corresponding to the pivotal interaction common to all the G-protein coupling aminergic receptors.<sup>[35]</sup>

Very interestingly, and not unexpectedly, imidazoline (S)-(+)-**19**, endowed with nanomolar affinity, is constantly (99%) anchored to the negatively charged head of Asp116, whereas (R)-(-)-**1** makes the same contact only in half of the MD trajectory. Anyway, water molecules assist the binding of both compounds through hydrogen-bond bridges with residues located

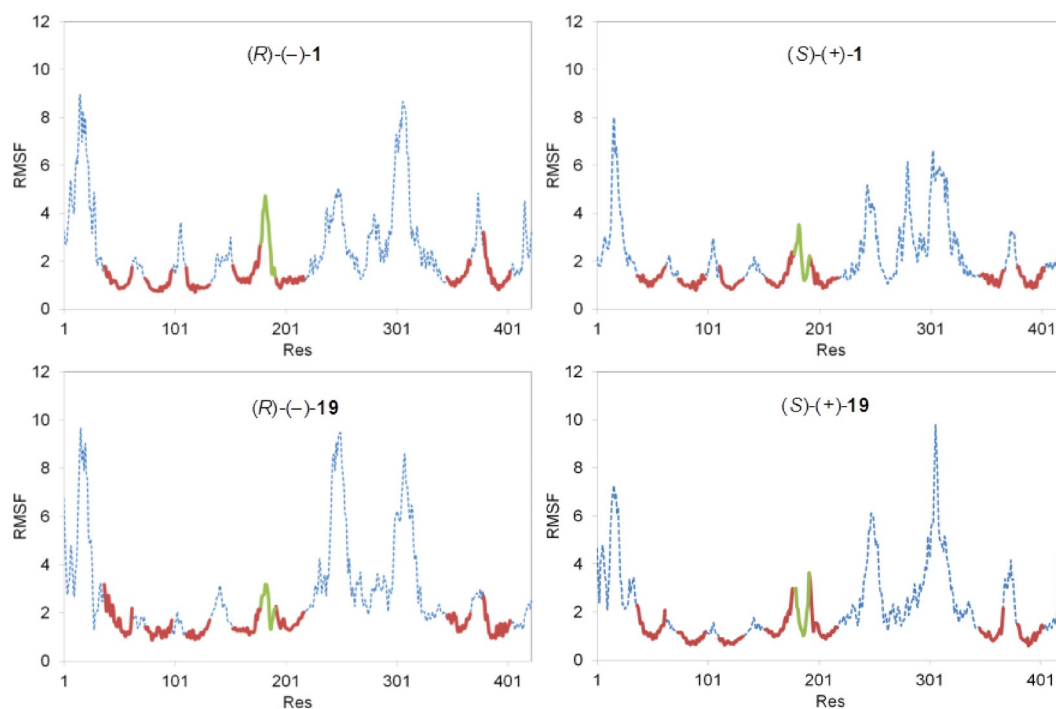


**Figure 3.** RMSF of the C $\alpha$  atoms of the whole 5-HT<sub>1A</sub>-R sequence (dashed blue line). The transmembrane domains and the second extracellular loop are represented by solid lines (red and green, respectively).

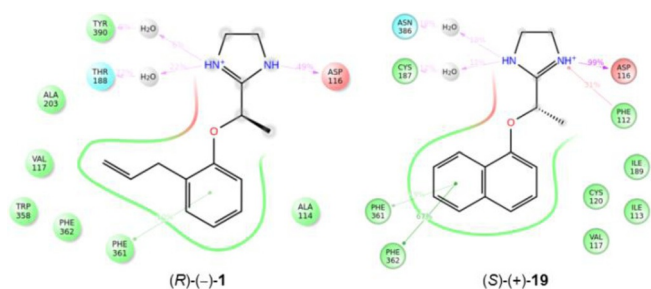


**Figure 4.** 2D protein–ligand interaction scheme for *(R)*-(-)-**1** and *(S)*-(+)-**19**. Bonds with a minimum contact strength more than 5% were calculated over the last 82 ns of the dynamic trajectory.

in the third (Cys187 and Thr188) and seventh transmembrane (Asn386 and Tyr390) domains. The merit of the same amino acids was proven by binding of serotonergic ligands with mutant receptors and SDM experiments.<sup>[36,37]</sup> Other interesting considerations might also be made on the role of the substituent. Indeed, the aromatic ring of *(S)*-(+)-**19**, which is deeply buried in the inner part of the sixth transmembrane helix, stabilizes strongly ligand binding; this results in  $\pi$ - $\pi$  stacking with the essential residues Phe361 and Phe362, which are part of the aromatic cluster most likely regulating receptor activation.<sup>[38]</sup> A similar observation cannot be made for the allyl moiety of *(R)*-(-)-**1**, which reproduces less-efficient hydrophobic interactions.

The last two issues relating structural and chemical properties to affinity might be illustrated by the binding pose of imidazoline *(S)*-(+)-**19** with the highest  $pK_i$  value (Figure 5). The complex endowing the lowest interaction energy between the ligand and the 5-HT<sub>1A</sub>-R surface suggested a plausible interpretation of the critical role of chirality and a polar function in the bridge. In eutomer *(S)*-(+)-**19**, the methyl group of the bridge points towards the aliphatic chain of Ile189, and in this way, the possibility to enlance the receptor surface is enhanced by this central and stereospecific interaction that can only take place in this configuration. Furthermore, as already assessed, the root-mean-square fluctuation (RMSF) of imidazoline

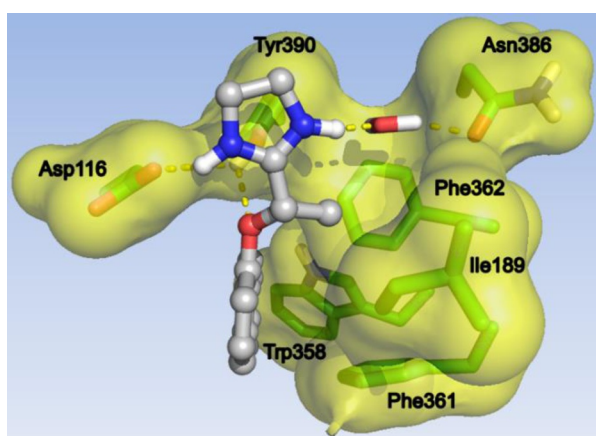


**Figure 5.** Representative pose of *(S)*-(+)-**19** into the human 5-HT<sub>1A</sub> binding site.

*(R)*-(-)-**1**, endowed with the lowest  $pK_i$  value, showed the most significant differences from the rest of the affine derivatives exactly in this region of the receptor, which suggests that during binding, the *R* configuration might disrupt some critical interactions essential for high affinity.

Finally, the need for a polar function emerged from the hydrogen bond made between the oxygen atom of the bridge and the hydroxy group of Tyr390; the same interaction would, of course, be absent in ligands characterized by a whole carbon spacer. Besides this qualitative interpretation of dockings, on the basis of the proof of concept of some essential interactions occurring in the receptor–ligand complex, such observations suggest that suitable chirality of the ligand and the size of its *ortho*-phenyl substituent can work in concert to favor 5-HT<sub>1A</sub>-R interaction.

### In vivo pharmacological studies

On the basis of the aforementioned involvement of 5-HT<sub>1A</sub>-R in depression,<sup>[13,15]</sup> we investigated the effect of new potent 5-HT<sub>1A</sub> full agonist **19** (named naphthylene) and its enantiomers on such emotional morbidity. Moreover, despite the high degree of homology between 5-HT<sub>1A</sub>-R and  $\alpha_1$ -ARs, **19**, examined in the present study according to previously reported procedures,<sup>[39]</sup> proved to be devoid of  $\alpha_1$ -AR affinity ( $pK_i < 6$ ). The antidepressant-like effects were examined by using the mice Porsolt test (forced swimming test) and are depicted in Figure 6.

Such methodology is widely used to predict antidepressant effects in humans. The mobility time of mice in the forced

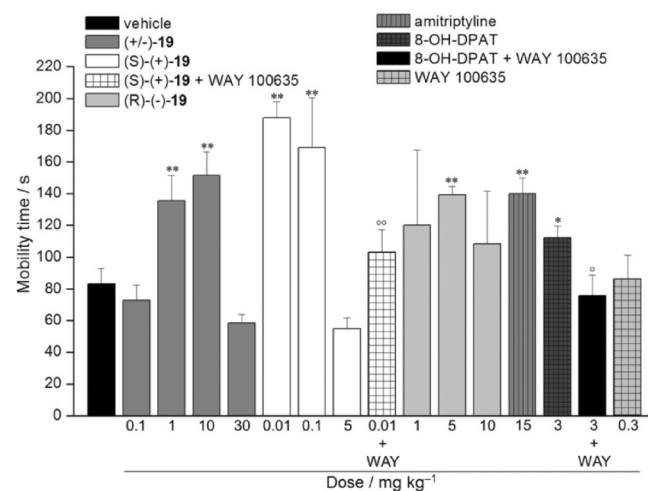


**Figure 6.** Antidepressant-like effects of  $(\pm)$ -**19** (0.1–30 mg kg<sup>-1</sup>), *(S)*-(+)-**19** (0.01–5 mg kg<sup>-1</sup>), and *(R)*-(-)-**19** (1–10 mg kg<sup>-1</sup>) in the mouse forced swimming test. The test was performed after a single administration p.o. of compounds at different dosages. Compounds were injected 26 min before the beginning of the experiment. Amitriptyline (15 mg kg<sup>-1</sup>, s.c.) was considered as reference drug. The 5-HT<sub>1A</sub> agonist 8-OH-DPAT (3 mg kg<sup>-1</sup> i.p.) and the antagonist WAY100635 (0.3 mg kg<sup>-1</sup>, s.c.) were used to study the pharmacodynamic mechanism. WAY100635 was injected 15 min before the administration of *(S)*-(+)-**19** or 8-OH-DPAT. Each value is the mean  $\pm$  SEM of 12 mice per group, performed in 2 different experimental sets. \* $P < 0.05$  and \*\* $P < 0.01$  versus vehicle treated animals; ° $P < 0.05$  and °° $P < 0.01$  versus the same treatment in the absence of WAY100635.

swimming test is increased by the majority of antidepressants, including tricyclic and atypical antidepressants, monoamine oxidase inhibitors, and 5-HT uptake inhibitors,<sup>[40]</sup> and their effectiveness significantly correlates with clinical potency.<sup>[41]</sup> Acute administration of **19** dosed at 1 and 10 mg kg<sup>-1</sup> per os (p.o.) was able to increase the mobility times to (135.0 ± 16.2) and (151.5 ± 15.0) s, respectively, in comparison with control animals treated with vehicle [(83.1 ± 9.8) s]. Doses of 0.1 and 30 mg kg<sup>-1</sup> were ineffective. Enantiomer (S)-(+)-**19**, endowed with very high 5-HT<sub>1A</sub>-R affinity (pK<sub>i</sub> = 8.89), showed a better antidepressant-like profile by increasing the mobility times up to (187.8 ± 10.3) and (169.2 ± 31.2) s dosed at 0.01 and 0.1 mg kg<sup>-1</sup>, respectively. On the contrary, (R)-(-)-**19** appeared fruitful at 5 mg kg<sup>-1</sup> only [(139.0 ± 5.5) s]. These results were compared with the effect induced by amitriptyline, a tricyclic antidepressant commonly used in human therapy.<sup>[42]</sup> Amitriptyline (15 mg kg<sup>-1</sup>, p.o.) increased the mobility time similarly to 1 mg kg<sup>-1</sup> of racemate **19**, and 5 mg kg<sup>-1</sup> of (R)-(-)-**19** but, interestingly, proved to be less efficacious and potent than (S)-(+)-**19**.

In the present study, we also confirmed the α<sub>2</sub>-AR agonist profile of **19**. In particular, the tests performed according to previously reported procedures on human α<sub>2</sub>-AR subtypes<sup>[6]</sup> indicated its preferential α<sub>2C</sub>-AR activation (pEC<sub>50</sub> α<sub>2A</sub> 5.4, ia. 0.5; pEC<sub>50</sub> α<sub>2B</sub> 5.2, ia. 0.4; pEC<sub>50</sub> α<sub>2C</sub> 7.11, ia. 0.8). On the other hand, as verified for **1** and its analogues, the 5-HT<sub>1A</sub>-R activation can favorably cooperate with α<sub>2C</sub>-AR stimulation in inducing antidepressant-like effect at low doses. The peculiar relationship between α<sub>2</sub>-AR activation and 5-HT function might explain the lack of antidepressant effect even at slightly higher doses, as we previously justified in ref. [11].

The antidepressant-like effect of (S)-(+)-**19** was significantly reduced by pretreatment with the 5-HT<sub>1A</sub>-R antagonist WAY100635, which demonstrated the involvement of 5-HT<sub>1A</sub>-R in the activity of (S)-(+)-**19**. WAY100635 per se did not induce any changes in mobility time relative to the control group. In comparison, the reference 5-HT<sub>1A</sub>-R agonist 8-OH-DPAT<sup>[43]</sup> was less potent and efficacious (Figure 6).

## Conclusions

According to previous results, the significant 5-HT<sub>1A</sub> receptor (5-HT<sub>1A</sub>-R) profile shown by several imidazoline compounds confirmed the bioversatility of the 2-substituted imidazoline nucleus and its ability to drive drugs towards 5-HT<sub>1A</sub>-R. The structure–activity relationships produced in the present investigation showed that the *ortho* substituent in the aromatic area, the nature of the bridge, and the chirality complemented each other to define the peculiar biological profile of the ligand. These observations, supported by modeling, might be particularly useful in the design of novel 5-HT<sub>1A</sub>-R ligands built on scaffold **I** reported in Figure 1. Interestingly, this study allowed identification of other ligands targeting 5-HT<sub>1A</sub>-R and highlighted the potent antidepressant-like effect provided by (S)-(+)-**19** [(S)-(+)-naphtyline] at the very low dose of 0.01 mg kg<sup>-1</sup>, clearly mediated by 5-HT<sub>1A</sub> as significantly reduced by pretreatment with the 5-HT<sub>1A</sub> antagonist WAY100635.

As is well known<sup>[44]</sup> and already verified by us,<sup>[11]</sup> α<sub>2</sub>-adrenergic receptor (α<sub>2</sub>-AR) stimulation can also cooperate to elicit an antidepressant effect. Nevertheless, as emerged from the present study, the very weak and partial α<sub>2A</sub>-AR agonism shown by (S)-(+)-**19** might induce minor side effects commonly associated with strong α<sub>2A</sub>-subtype activation and observed with the use of full α<sub>2A</sub>-AR agonists such as clonidine and clonidine-like drugs. Interestingly, despite the high degree of homology between 5-HT<sub>1A</sub>-R and α<sub>1</sub>-ARs, **19** was devoid of α<sub>1</sub>-AR affinity.

## Experimental Section

### Chemistry

Melting points were taken in glass capillary tubes with a Büchi SMP-20 apparatus and are uncorrected. IR and NMR spectra were recorded with PerkinElmer 297 and Varian Mercury AS400 instruments, respectively. Chemical shifts are reported in parts per million (ppm) relative to tetramethylsilane, and spin multiplicities are given as s (singlet), d (doublet), dd (doublet of doublets), t (triplet), q (quartet), and m (multiplet). IR spectral data (not shown because of the lack of unusual features) were obtained for all compounds reported and are consistent with the assigned structures. The microanalyses were recorded with a FLASH 2000 instrument (ThermoFisher Scientific). The elemental compositions of the compounds agreed to within ± 0.4% of the calculated values. Optical rotation was measured at a 1 g/100 mL concentration (c = 1) with a PerkinElmer 241 polarimeter (accuracy ± 0.002°). Chromatographic separations were performed on silica-gel columns (Kieselgel 40, 0.040–0.063 mm, Merck) by flash chromatography. Compounds were named following IUPAC rules as applied by ChemBioDraw Ultra (version 11.0) software for systematically naming organic chemicals. The purities of the novel compounds were determined by combustion analysis and were ≥ 95%.

### Synthesis

**2-[1-(Naphthalen-1-yloxy)ethyl]-4,5-dihydro-1H-imidazole (19)**: A solution of ethylenediamine (0.47 mL, 6.5 mmol) in dry toluene (9 mL) was added dropwise to a stirred solution of 2 M trimethylaluminum (3.5 mL, 6.5 mmol) in dry toluene (5 mL) at 0 °C under a nitrogen atmosphere, and the mixture was stirred at room temperature for 1 h. The solution was cooled to 0 °C, and a solution of **62** (0.71 g, 3.5 mmol) in dry toluene (8 mL) was added dropwise. The mixture was heated to reflux for 20 h, cooled to 0 °C, and quenched cautiously with MeOH (0.8 mL) followed by H<sub>2</sub>O (0.25 mL). After the addition of CHCl<sub>3</sub> (11.0 mL), the mixture was stirred for 30 min at 55 °C to ensure precipitation of the aluminum salts. The mixture was filtered, and the organic layer was extracted with 2 N HCl. The aqueous layer was made basic with 10% NaOH and was extracted with CHCl<sub>3</sub>. The organic layer was dried with Na<sub>2</sub>SO<sub>4</sub>, filtered, and concentrated to give a residue, which was purified by flash chromatography (EtOAc/MeOH/33% NH<sub>4</sub>OH 8:2:0.1) to obtain an oil (0.42 g, 51% yield). <sup>1</sup>H NMR (CDCl<sub>3</sub>): δ = 1.74 (d, 3H, CH<sub>3</sub>CH), 3.42–3.76 (m, 4H, NCH<sub>2</sub>CH<sub>2</sub>N), 4.49 (brs, 1H, NH, exchangeable with D<sub>2</sub>O), 5.24 (q, 1H, CH<sub>2</sub>CH), 6.94 (d, 1H, ArH), 7.31–7.54 (m, 4H, ArH), 7.80 (m, 1H, ArH), 8.26 ppm (m, 1H, ArH). The free base was transformed into the oxalate salt, which was crystallized from EtOH: mp: 167–169 °C. Elemental analysis calcd (%) for C<sub>15</sub>H<sub>16</sub>N<sub>2</sub>O·C<sub>2</sub>H<sub>2</sub>O<sub>4</sub> (330.34): C 61.81, H 5.49, N 8.48; found: C 61.94, H 5.56, N 8.30.



**Resolution of 2-[1-(Naphthalen-1-yloxy)ethyl]-4,5-dihydro-1H-imidazole (19):** Racemic **19** (1 g, 4.16 mmol) in EtOH (30 mL) was treated with a solution of (+)-*O,O'*-dibenzoyl-D-tartaric acid (1.49 g, 4.16 mmol) in EtOH (35 mL), and the mixture was left at room temperature for 30 h. White crystals were crystallized twice from EtOH: 0.9 g yield. The salt was dissolved in water (50 mL), and the ice-cooled solution was made basic with 2 N NaOH and extracted with EtOAc (3 × 30 mL). Removal of the dried solvent gave (*S*)-(+)-**19**; yield: 0.34 g. The <sup>1</sup>H NMR spectrum was identical to that of **19**. The enantiomeric purity, determined by <sup>1</sup>H NMR spectroscopy upon the addition of (*S*)-(+)-2,2,2-trifluoro-1-(9-anthryl)ethanol as a chiral shift reagent, was >98%. The free base was transformed into the oxalate salt, which was crystallized from EtOH: mp: 167–169 °C. [ $\alpha$ ]<sub>D</sub><sup>20</sup> = +123.4 (*c* = 1 in CH<sub>3</sub>OH). Elemental analysis calcd (%) for C<sub>15</sub>H<sub>16</sub>N<sub>2</sub>O·C<sub>2</sub>H<sub>2</sub>O<sub>4</sub> (330.34): C 61.81, H 5.49, N 8.48; found: C 61.91, H 5.60, N 8.27.

Similar treatment of **19** with (–)-*O,O'*-dibenzoyl-L-tartaric acid gave enantiomer (*R*)-(–)-**19**, the <sup>1</sup>H NMR spectrum of which was identical to that of **19**. The enantiomeric purity, determined by <sup>1</sup>H NMR spectroscopy upon the addition of (*S*)-(+)-2,2,2-trifluoro-1-(9-anthryl)ethanol as a chiral shift reagent, was >98%. The free base was transformed into the oxalate salt, which was crystallized from EtOH: mp: 167–169 °C. [ $\alpha$ ]<sub>D</sub><sup>20</sup> = –122.8 (*c* = 1 in CH<sub>3</sub>OH). Elemental analysis calcd (%) for C<sub>15</sub>H<sub>16</sub>N<sub>2</sub>O·C<sub>2</sub>H<sub>2</sub>O<sub>4</sub> (330.34): C 61.81, H 5.49, N 8.48; found: C 61.96, H 5.65, N 8.23.

**(S)-(+)-2-[1-(Naphthalen-1-yloxy)ethyl]-4,5-dihydro-1H-imidazole [(S)-(+)-19]:** This compound was prepared starting from (*S*)-(+)-**62** by following the procedure described for **19** by heating the mixture to 65 °C for 5 h; an oil was obtained (47% yield). The <sup>1</sup>H NMR spectrum was identical to that of **19**. The enantiomeric purity, determined by <sup>1</sup>H NMR spectroscopy upon the addition of (*S*)-(+)-2,2,2-trifluoro-1-(9-anthryl)ethanol as a chiral shift reagent, was approximately 85%.

**(R)-(–)-2-[1-(Naphthalen-1-yloxy)ethyl]-4,5-dihydro-1H-imidazole [(R)-(–)-19]:** This compound was prepared starting from (*R*)-(–)-**62** by following the procedure described for **19** by heating the mixture to 65 °C for 5 h; an oil was obtained (47% yield). The <sup>1</sup>H NMR spectrum was identical to that of **19**. The enantiomeric purity, determined by <sup>1</sup>H NMR spectroscopy upon the addition of (*S*)-(+)-2,2,2-trifluoro-1-(9-anthryl)ethanol as a chiral shift reagent, was approximately 85%.

**3-[2-[(4,5-Dihydro-1H-imidazol-2-yl)methoxy]phenyl]pyridine (31):** A mixture of ethylenediamine (2.0 g, 33.3 mmol) and **60** (0.68 g, 3.26 mmol) was heated at reflux for 20 h. After cooling and adding H<sub>2</sub>O (30 mL), the mixture was extracted with CHCl<sub>3</sub> (3 × 20 mL). The organic layer was washed with H<sub>2</sub>O (2 × 20 mL), dried with Na<sub>2</sub>SO<sub>4</sub>, and concentrated to give a residue, which was purified by flash chromatography (EtOAc/MeOH/33% NH<sub>4</sub>OH 95:5:0.1) to obtain an oil (0.64 g, 78% yield). <sup>1</sup>H NMR (CDCl<sub>3</sub>):  $\delta$  = 3.42–3.83 (m, 4H, NCH<sub>2</sub>CH<sub>2</sub>N), 4.78 (s, 2H, OCH<sub>2</sub>), 4.90 (brs, 1H, NH, exchangeable with D<sub>2</sub>O), 7.01–7.23 (m, 5H, ArH), 7.80 (d, 1H, ArH), 8.53 (d, 1H, ArH), 8.87 ppm (s, 1H, ArH). The free base was transformed into the oxalate salt, which was crystallized from EtOH: mp: 152–153 °C. Elemental analysis calcd (%) for C<sub>15</sub>H<sub>15</sub>N<sub>3</sub>O·C<sub>2</sub>H<sub>2</sub>O<sub>4</sub> (343.33): C 59.47, H 4.99, N 12.24; found: C 59.20, H 5.12, N 12.03.

**2-[(3'-Fluoro-[1,1'-biphenyl]-2-yl)oxy)methyl]-4,5-dihydro-1H-imidazole (33):** This compound was prepared starting from **61** by following the procedure described for **31**; an oil was obtained (64% yield). <sup>1</sup>H NMR (CDCl<sub>3</sub>):  $\delta$  = 3.59 (m, 4H, NCH<sub>2</sub>CH<sub>2</sub>N), 4.70 (s, 2H, OCH<sub>2</sub>), 4.95 (brs, 1H, NH, exchangeable with D<sub>2</sub>O), 6.98–7.38 ppm (m, 8H, ArH). The free base was transformed into the ox-

alate salt, which was crystallized from EtOH: mp: 150–153 °C. Elemental analysis calcd (%) for C<sub>16</sub>H<sub>15</sub>FN<sub>2</sub>O·C<sub>2</sub>H<sub>2</sub>O<sub>4</sub> (360.34): C 60.00, H 4.76, N 7.77; found: C 59.79, H 4.92, N 7.89.

**2-(2-Allylphenethyl)-4,5-dihydro-1H-imidazole (46):** This compound was prepared starting from **58**<sup>[30]</sup> by following the procedure described for **19** by heating the mixture to 65 °C for 5 h; an oil was obtained (56% yield). <sup>1</sup>H NMR (CDCl<sub>3</sub>):  $\delta$  = 2.54 (t, 2H, CH<sub>2</sub>CH<sub>2</sub>), 2.99 (t, 2H, CH<sub>2</sub>CH<sub>2</sub>), 3.25 (d, 2H, CH<sub>2</sub>Ar), 3.71 (m, 4H, NCH<sub>2</sub>CH<sub>2</sub>N), 4.73 (brs, 1H, NH, exchangeable with D<sub>2</sub>O), 5.00 (m, 2H, CH<sub>2</sub>=CH), 6.01 (m, 1H, CH<sub>2</sub>=CH), 7.15–7.25 ppm (m, 4H, ArH). The free base was transformed into the oxalate salt, which was crystallized from EtOH: mp: 137–139 °C. Elemental analysis calcd (%) for C<sub>14</sub>H<sub>18</sub>N<sub>2</sub>·C<sub>2</sub>H<sub>2</sub>O<sub>4</sub> (304.34): C 63.14, H 6.62, N 9.20; found: C 63.32, H 6.44, N 9.01.

**2-[2-(Cyclopropylmethyl)phenethyl]-4,5-dihydro-1H-imidazole (47):** This compound was prepared starting from **59** by following the procedure described for **19**; an oil was obtained (64% yield). <sup>1</sup>H NMR (CDCl<sub>3</sub>):  $\delta$  = 0.19 (m, 2H, cyclopropyl), 0.48 (m, 2H, cyclopropyl), 0.97 (m, 1H, cyclopropyl), 2.60 (d, 2H, CH<sub>2</sub>Ar), 2.68 (t, 2H, CH<sub>2</sub>CH<sub>2</sub>), 2.90 (t, 2H, CH<sub>2</sub>CH<sub>2</sub>), 3.82 (m, 4H, NCH<sub>2</sub>CH<sub>2</sub>N), 4.54 (brs, 1H, NH, exchangeable with D<sub>2</sub>O), 7.15–7.61 ppm (m, 4H, ArH). The free base was transformed into the oxalate salt, which was crystallized from EtOH: mp: 140–141 °C. Elemental analysis calcd (%) for C<sub>15</sub>H<sub>20</sub>N<sub>2</sub>·C<sub>2</sub>H<sub>2</sub>O<sub>4</sub> (318.37): C 64.13, H 6.97, N 8.80; found: C 63.98, H 7.11, N 8.95.

**2-(Cyclopropylmethyl)benzaldehyde (56):** Et<sub>2</sub>Zn (1.0 M in hexanes, 20 mL, 20 mmol) was added to freshly distilled CH<sub>2</sub>Cl<sub>2</sub> (20 mL) under an atmosphere of N<sub>2</sub>. A solution of trifluoroacetic acid (1.54 mL, 20 mmol) in CH<sub>2</sub>Cl<sub>2</sub> (10 mL) was added dropwise by syringe into the mixture cooled in an ice bath. Upon stirring for 20 min, a solution of CH<sub>2</sub>I<sub>2</sub> (1.61 mL, 20 mmol) in CH<sub>2</sub>Cl<sub>2</sub> (10 mL) was added. After stirring for an additional 20 min, a solution of 2-allylbenzaldehyde (1.46 g, 10.0 mmol) in CH<sub>2</sub>Cl<sub>2</sub> (10 mL) was added, and the ice bath was removed. After stirring for an additional 30 min, the mixture was quenched with 0.1 N HCl (50 mL) and Et<sub>2</sub>O (25 mL), and the layers were separated. The aqueous layer was extracted with hexanes. The combined organic layer was dried with anhydrous Na<sub>2</sub>SO<sub>4</sub>, filtered, concentrated, and purified by column chromatography (cyclohexane/EtOAc 95:5) to obtain an oil (0.72 g; 45% yield). <sup>1</sup>H NMR (CDCl<sub>3</sub>):  $\delta$  = 0.20 (m, 2H, cyclopropyl), 0.51 (m, 2H, cyclopropyl), 1.02 (m, 1H, cyclopropyl), 2.99 (d, 2H, CH<sub>2</sub>Ar), 7.23 (d, 1H, ArH), 7.33 (t, 1H, ArH), 7.50 (t, 1H, ArH), 7.92 (d, 1H, ArH), 10.23 ppm (s, 1H, CHO).

**Methyl 3-[2-(cyclopropylmethyl)phenyl]acrylate (57):** A solution of methyl 2-(diethoxyphosphoryl)acetate (0.34 g, 1.62 mmol) in THF (5 mL) was added dropwise to a suspension of NaH (0.65 g, 2.71 mmol) in THF (5 mL) at 0 °C under an atmosphere of N<sub>2</sub>. After 30 min, a solution of **56** (0.22 g, 1.37 mmol) in THF (2 mL) was added dropwise. The mixture was stirred at RT for 3 h, cooled to 0 °C, and quenched with an excess amount of H<sub>2</sub>O. Then, it was extracted with EtOAc (3 × 20 mL), and the organic layer was dried with Na<sub>2</sub>SO<sub>4</sub>. Removal of the solvent gave a residue that was purified by column chromatography (cyclohexane/EtOAc 98:2) to obtain an oil (0.22 g; 75% yield). <sup>1</sup>H NMR (CDCl<sub>3</sub>):  $\delta$  = 0.18 (m, 2H, cyclopropyl), 0.46 (m, 2H, cyclopropyl), 0.91 (m, 1H, cyclopropyl), 2.66 (d, 2H, CH<sub>2</sub>Ar), 3.91 (s, 3H, OCH<sub>3</sub>), 6.28 (d, 1H, CH=CH), 7.20–7.28 (m, 3H, ArH), 7.49 (d, 1H, ArH), 8.02 ppm (d, 1H, CH=CH).

**Methyl 3-[2-(cyclopropylmethyl)phenyl]propanoate (59):** 10% Pd/C (0.4 g) was added portionwise to a solution of **57** (1.0 g, 4.63 mmol) in CH<sub>3</sub>OH (10 mL). The mixture was hydrogenated at 0.34 MPa for 20 h at room temperature. Following catalyst removal,

evaporation of the solvent gave a residue that was purified by column chromatography (cyclohexane/EtOAc 98:2) to obtain an oil (0.72 g, 68% yield).  $^1\text{H NMR}$  ( $\text{CDCl}_3$ ):  $\delta$  = 0.19 (m, 2H, cyclopropyl), 0.49 (m, 2H, cyclopropyl), 0.95 (m, 1H, cyclopropyl), 2.57 (m, 4H,  $\text{CH}_2\text{CH}_2$  e  $\text{CH}_2\text{Ar}$ ), 2.97 (t, 2H,  $\text{CH}_2\text{CH}_2$ ), 3.84 (s, 3H,  $\text{OCH}_3$ ), 7.17–7.27 ppm (m, 4H, ArH).

**2-[2-(Pyridin-3-yl)phenoxy]acetonitrile (60):** 3-Pyridylboronic acid (0.60 g, 4.88 mmol), tetrakis(triphenylphosphine)palladium(0) (0.22 g, 0.19 mmol), and 2M  $\text{Na}_2\text{CO}_3$  (0.97 g, 9.15 mmol) were added to a solution of 2-(2-bromophenoxy)acetonitrile<sup>[31]</sup> (0.82 g, 3.90 mmol) in DME (10 mL). The mixture was heated at reflux in a dark box under an atmosphere of  $\text{N}_2$  for 20 h. Then, it was poured into  $\text{H}_2\text{O}$  (30 mL) and EtOAc (3  $\times$  20 mL); the organic layer was washed with iced  $\text{H}_2\text{O}$  and dried with  $\text{Na}_2\text{SO}_4$ . Removal of the solvent gave a residue that was purified by column chromatography (cyclohexane/EtOAc 9:1) to obtain an oil (0.65 g, 80% yield).  $^1\text{H NMR}$  ( $\text{CDCl}_3$ ):  $\delta$  = 4.68 (s, 2H,  $\text{OCH}_2$ ), 7.08–7.42 (m, 5H, ArH), 7.82 (d, 1H, ArH), 8.59 (d, 1H, ArH), 8.66 ppm (s, 1H, ArH).

**2-[(3'-Fluoro-[1,1'-biphenyl]-2-yl)oxy]acetonitrile (61):** This compound was prepared starting from 2-(2-bromophenoxy)acetonitrile (0.82 g, 3.90 mmol)<sup>[31]</sup> and 3-fluorophenylboronic acid (0.68 g, 4.88 mmol) following the procedure described for **60**; an oil was obtained (80% yield).  $^1\text{H NMR}$  ( $\text{CDCl}_3$ ):  $\delta$  = 4.65 (s, 2H,  $\text{OCH}_2$ ), 7.01–7.39 ppm (m, 8H, ArH).

**Methyl 2-(naphthalen-1-yloxy)propanoate (62):** A mixture of naphthalen-1-ol (1.67 g, 11.6 mmol), methyl 2-bromopropionate (1.74 g, 11.6 mmol), and  $\text{K}_2\text{CO}_3$  (1.60 g, 11.6 mmol) in DME (10 mL) was heated at reflux for 18 h. The mixture was cooled and filtered. The solvent was removed under reduced pressure to give a residue, which was taken up in  $\text{CH}_2\text{Cl}_2$  (30 mL) and washed with cold 2N NaOH (2  $\times$  20 mL). Removal of the solvent afforded an oil that was purified by flash chromatography (cyclohexane/EtOAc 98:2) to obtain an oil (2.32 g; 87% yield).  $^1\text{H NMR}$  ( $\text{CDCl}_3$ ):  $\delta$  = 1.77 (d, 3H,  $\text{CH}_3\text{CH}$ ), 3.76 (s, 3H,  $\text{OCH}_3$ ), 4.96 (q, 1H,  $\text{CH}_3\text{CH}$ ), 6.69 (d, 1H, ArH), 7.29–7.57 (m, 4H, ArH), 7.80 (m, 1H, ArH), 8.36 ppm (m, 1H, ArH).

**(S)-(+)-Methyl 2-(naphthalen-1-yloxy)propanoate [(S)-(+)-62]:** A solution of DIAD (3.01 g, 14.9 mmol) in dry THF (10 mL) was added dropwise to a mixture of methyl (*R*)-(+)-lactate (1.36 g, 13.1 mmol), naphthalen-1-ol (1.83 g, 12.7 mmol), and triphenylphosphine (3.34 g, 12.7 mmol) in THF (20 mL). The mixture was stirred at room temperature overnight under an atmosphere of  $\text{N}_2$ . The solvent was evaporated, and diethyl ether/hexane (20 mL, 1:1) was added. The triphenylphosphine oxide precipitate was filtered off, and removal of the dried solvent gave a residue that was purified by flash chromatography (cyclohexane/EtOAc 95:5) to obtain an oil (52% yield). The  $^1\text{H NMR}$  spectrum was identical to that of **62**.  $[\alpha]_D^{20} = +26.2$  ( $c = 1$  in  $\text{CHCl}_3$ ).

**(R)-(–)-Methyl 2-(naphthalen-1-yloxy)propanoate [(R)-(–)-62]:** This compound was prepared starting from methyl (*S*)-(–)-lactate following the procedure described for (*S*)-(+)-**62**; an oil was obtained (50% yield). The  $^1\text{H NMR}$  spectrum was identical to that of **62**.  $[\alpha]_D^{20} = -26.6$  ( $c = 1$  in  $\text{CHCl}_3$ ).

### Molecular modeling

The molecular scaffolds of the ligands in their ionized forms with standard bond lengths and valence angles were achieved upon AM1 minimization with the NDDO semiempirical tool implemented in the Maestro software package.<sup>[45]</sup>

For comparative building of the 5-HT<sub>1A</sub> receptor, the crystallographic coordinates of the chimera complex of human 5-HT<sub>1B</sub> with the serotonergic agonist ergotamine (PDB ID: 4IAR) were selected as a template having a high ( $\approx 60\%$ ) degree of homology with the query sequence. A CLUSTAL sequence alignment (scoring matrix = PAM350, gap open penalty = 10, gap extension penalty = 0.1) (Figure S1, Supporting Information) was generated to achieve thereafter a former set of molecular scaffolds of 5-HT<sub>1A</sub> by means of MODELLER ver 9.15 software.<sup>[46]</sup> In total, 500 models were firstly achieved, and starting from the best scaffold, according to the discrete optimized protein energy (DOPE) scoring function implemented in MODELLER, another 500 models were generated by refining the lone loop regions with the *refine\_slow* routine. The stereochemical parameters were checked with PROCHECK,<sup>[47]</sup> and having proved that more than 90% of the receptor residues resulted in the core region of the Ramachandran plot, the structure was passed to the Protein Preparation Wizard implemented in MAESTRO, for which all the hydrogen atoms were added and their positions refined.

The input structures for dynamics runs were generated by superimposing ligands with the shape-based matching algorithm ROCS<sup>[48]</sup> to X-ray conformation of ergotamine, and then docking the highest Tanimoto coefficient pose with AUTODOCK ver. 4.2.<sup>[49]</sup>

For 5-HT<sub>1A</sub>-R electrostatic charges were assigned by means of the AUTODOCK TOOLS<sup>[50]</sup> according to the AMBER UNITED force field.<sup>[51]</sup>

Affinity maps were calculated by AUTOGRID by using a 75  $\times$  65  $\times$  65 rectangular box with a spacing of 0.375 Å centered on the center of mass of a binding site comprising residues Asp116, Trp358, Phe361, Phe362, Asn386, and Tyr390. The conformational space was explored with the Lamarckian Genetic Algorithm by randomly translating and perturbing ligands in a total of 250 runs of docking by assigning flexibility to the side chains of the previously mentioned amino acids.

The achieved receptor–ligand complex served as an input structure for subsequent molecular dynamics performed with Desmond.<sup>[52]</sup>

The same complex was assembled by using the Desmond system builder tool implemented in Maestro<sup>[53]</sup> by embedding the protein in a palmitoyl-oleoyl-phosphatidyl-choline lipid bilayer spanning the seven transmembrane helices (namely, residues 37–62, 74–98, 111–132, 153–178, 192–217, 346–367, and 379–403) and neutralizing the whole system with  $\text{Na}^+$  and  $\text{Cl}^-$  counterions. The achieved molecular assembly was first minimized by fixing the C $\alpha$  trace atoms with a harmonic constant of 100 kcal mol<sup>-1</sup> Å<sup>-2</sup> until an convergence gradient threshold of 1.0 kcal mol<sup>-1</sup> and was then subjected to stochastic dynamics at constant temperature (300 K) and pressure (0.1 MPa) for a total of 96 ns by using the default settings of Desmond. Energy and trajectory data were recorded every 1.2 ps.

### In vivo pharmacological studies

**Animals:** Male CD-1 albino mice (Harlan, Varese, Italy) weighing approximately 22–25 g at the beginning of the experimental procedure were used. Animals were housed in CeSAL (Centro Stabulazione Animali da Laboratorio, University of Florence) and were used at least 1 week after their arrival. Twelve mice were housed per cage (size 26  $\times$  41 cm); animals were fed a standard laboratory diet and tap water ad libitum and were kept at (23  $\pm$  1) °C with a 12 h light/dark cycle, light at 7 a.m. All animal manipulations were performed according to the European Community guidelines

for animal care (DL 116/92), application of the European Communities Council Directive of 24 November 1986 (86/609/EEC). The ethical policy of the University of Florence complies with the Guide for the Care and Use of Laboratory Animals of the US National Institutes of Health (NIH Publication No. 85–23, revised 1996; University of Florence assurance number: A5278–01). Formal approval to conduct the experiments described was obtained from the Animal Subjects Review Board of the University of Florence. Experiments involving animals were reported according to ARRIVE guidelines.<sup>[54]</sup> All efforts were made to minimize animal suffering and to reduce the number of animals used.

**Pharmacological treatments:** To evaluate the antidepressant-like activity, **19** (0.1–30 mg kg<sup>-1</sup>), (S)-(+)-**19** (0.01–5 mg kg<sup>-1</sup>), and (R)-(–)-**19** (1–10 mg kg<sup>-1</sup>) were suspended in 1% carboxymethyl cellulose and p.o. administered 26 min before the beginning of the test. Amitriptyline [15 mg kg<sup>-1</sup>, subcutaneous (s.c.) in saline solution] and 8-OH-DPAT [3 mg kg<sup>-1</sup>, intraperitoneal (i.p.) in saline solution] were used as reference compounds. WAY100635 (0.3 mg kg<sup>-1</sup>) was injected s.c. 15 min before the administration of (S)-(+)-**19** or 8-OH-DPAT. The doses of amitriptyline, 8-OH-DPAT, and WAY100635 were chosen on the basis of previously published data.<sup>[42,43,55,56]</sup> The volume administered was 0.1 mL/10 g body weight.

**Forced swimming test:** The forced swimming test used was the same as that described by Porsolt et al.<sup>[57]</sup> Briefly, mice were placed individually into glass cylinders (height: 25 cm, diameter: 10 cm) containing 12 cm of water maintained at 22–23 °C and were left there for 6 min. A mouse was judged to be immobile if it floated in the water, in an upright position, and made only small movements to keep its head above water. The duration of mobility was recorded during the last 4 min of the 6 min test. An increase in the duration of mobility was indicative of an antidepressant-like effect. Twelve mice per group were tested.

**Statistical analysis:** Behavioral measurements were performed on 12 mice for each treatment performed in two different experimental sets. Standard ANOVA followed by Fisher's protected least significant difference procedure were used. Results were expressed as the means ± SEM. All assessments were made by researchers blinded to cell or rat treatments. Data were analyzed by using the Origin 8.1 software (OriginLab, Northampton, USA).

### Abbreviations

5-HT, 5-hydroxytryptamine; 5-HT<sub>1A</sub>-R, 5-HT<sub>1A</sub> receptor; α-AR, α-adrenergic receptor; CCI, chronic constriction injury; ee, enantiomeric excess; FEB, free energy of binding; IBS, imidazoline binding sites; i.p., intraperitoneal; MD, molecular dynamics; p.o., per os; SAR, structure-activity relationship; SDM, molecular dynamic simulation; s.c., subcutaneous.

### Acknowledgements

This work was supported by a grant from the University of Camerino (Fondo di Ateneo la Ricerca 2014–2015). The authors express their gratitude to Rosanna Matucci (University of Florence), Andrea Mazzanti (University of Bologna), and Rosanna Lovallo (University of Bari) for their useful suggestions.

**Keywords:** antidepressant agents • drug design • nitrogen heterocycles • receptors • serotonin receptor agonists

- [1] C. Dardonville, I. Rozas, *Med. Res. Rev.* **2004**, *24*, 639–661.
- [2] G. A. Head, D. N. Mayorov, *Cardiovasc. Hematol. Agents Med. Chem.* **2006**, *4*, 17–32.
- [3] M. Krasavin, *Eur. J. Med. Chem.* **2015**, *97*, 525–537.
- [4] F. Gentili, P. Bousquet, L. Brasili, M. Dontenwill, J. Feldman, F. Ghelfi, M. Giannella, A. Piergentili, W. Quaglia, M. Pignini, *J. Med. Chem.* **2003**, *46*, 2169–2176.
- [5] F. Del Bello, E. Diamanti, M. Giannella, V. Mammoli, L. Mattioli, F. Titomanlio, A. Piergentili, W. Quaglia, M. Lanza, C. Sabatini, G. Caselli, E. Poggesi, M. Pignini, *ACS Med. Chem. Lett.* **2013**, *4*, 875–879 and references cited therein.
- [6] F. Gentili, F. Ghelfi, M. Giannella, A. Piergentili, M. Pignini, W. Quaglia, C. Vesprini, P.-A. Crassous, H. Paris, A. Carrieri, *J. Med. Chem.* **2004**, *47*, 6160–6173.
- [7] F. Gentili, C. Cardinaletti, C. Vesprini, A. Carrieri, F. Ghelfi, A. Farande, M. Giannella, A. Piergentili, W. Quaglia, J. M. Laurila, A. Huhtinen, M. Scheinin, M. Pignini, *J. Med. Chem.* **2008**, *51*, 4289–4299 and references cited therein.
- [8] C. Cardinaletti, L. Mattioli, F. Ghelfi, F. Del Bello, M. Giannella, A. Bruzzone, H. Paris, M. Perfumi, A. Piergentili, W. Quaglia, M. Pignini, *J. Med. Chem.* **2009**, *52*, 7319–7322 and references cited therein.
- [9] F. Del Bello, L. Mattioli, F. Ghelfi, M. Giannella, A. Piergentili, W. Quaglia, C. Cardinaletti, M. Perfumi, R. J. Thomas, U. Zanelli, C. Marchioro, M. Dal Cin, M. Pignini, *J. Med. Chem.* **2010**, *53*, 7825–7835.
- [10] E. Diamanti, F. Del Bello, G. Carbonara, A. Carrieri, G. Fracchiolla, M. Giannella, V. Mammoli, A. Piergentili, K. Pohjanoksa, W. Quaglia, M. Schenin, M. Pignini, *Bioorg. Med. Chem.* **2012**, *20*, 2082–2090.
- [11] F. Del Bello, E. Diamanti, M. Giannella, V. Mammoli, C. Marchioro, L. Mattioli, F. Titomanlio, A. Piergentili, W. Quaglia, M. Varrone, M. Pignini, *ACS Med. Chem. Lett.* **2012**, *3*, 535–539.
- [12] M. Ubaldi, F. Del Bello, E. Domi, M. Pignini, C. Nasuti, *Eur. J. Pharmacol.* **2015**, *760*, 122–128.
- [13] F. Fiorino, B. Severino, E. Magli, A. Ciano, G. Caliendo, V. Santagada, F. Frecentese, E. Perisutti, *J. Med. Chem.* **2014**, *57*, 4407–4426.
- [14] S. Kalipatnapu, A. Chattopadhyay, *Cell. Mol. Neurobiol.* **2007**, *27*, 1097–1116.
- [15] S. Wieland, I. Lucki, *Psychopharmacology* **1990**, *101*, 497–504.
- [16] L. Citrome, *Int. J. Clin. Pract.* **2012**, *66*, 356–368.
- [17] a) M. Toth, *Eur. J. Pharmacol.* **2003**, *463*, 177–184; b) H. Kuserow, B. Davies, H. Hörtnagl, I. Voigt, T. Stroh, B. Bert, D. R. Deng, H. Fink, R. W. Veh, F. Theuring, *Mol. Brain Res.* **2004**, *129*, 104–116.
- [18] E. Lacivita, M. Leopoldo, F. Berardi, R. Perrone, *Curr. Top. Med. Chem.* **2008**, *8*, 1024–1034.
- [19] D. E. Nichols, C. D. Nichols, *Chem. Rev.* **2008**, *108*, 1614–1641.
- [20] F. Del Bello, V. Bargelli, C. Cifani, P. Gratteri, C. Bazzicalupi, E. Diamanti, M. Giannella, V. Mammoli, R. Matucci, M. V. Micioni Di Bonaventura, A. Piergentili, W. Quaglia, M. Pignini, *ACS Med. Chem. Lett.* **2015**, *6*, 496–501 and references cited therein.
- [21] F. Gentili, C. Cardinaletti, A. Carrieri, F. Ghelfi, L. Mattioli, M. Perfumi, C. Vesprini, M. Pignini, *Eur. J. Pharmacol.* **2006**, *553*, 73–81 and references cited therein.
- [22] F. Gentili, P. Bousquet, L. Brasili, M. Caretto, A. Carrieri, M. Dontenwill, M. Giannella, G. Marucci, M. Perfumi, A. Piergentili, W. Quaglia, C. Rascente, M. Pignini, *J. Med. Chem.* **2002**, *45*, 32–40 and references cited therein.
- [23] F. Gentili, C. Cardinaletti, C. Vesprini, F. Ghelfi, A. Farande, M. Giannella, A. Piergentili, W. Quaglia, L. Mattioli, M. Perfumi, A. Hudson, M. Pignini, *J. Med. Chem.* **2008**, *51*, 5130–5134 and references cited therein.
- [24] M. Pignini, P. Bousquet, A. Carotti, M. Dontenwill, M. Giannella, R. Moriconi, A. Piergentili, W. Quaglia, S. K. Tayebati, L. Brasili, *Bioorg. Med. Chem.* **1997**, *5*, 833–841 and references cited therein.
- [25] M. Pignini, P. Bousquet, L. Brasili, A. Carrieri, R. Cavagna, M. Dontenwill, F. Gentili, M. Giannella, F. Leonetti, A. Piergentili, W. Quaglia, A. Carotti, *Bioorg. Med. Chem.* **1998**, *6*, 2245–2260.
- [26] P.-A. Crassous, C. Cardinaletti, A. Carrieri, B. Bruni, M. Di Vaira, F. Gentili, F. Ghelfi, M. Giannella, H. Paris, A. Piergentili, W. Quaglia, S. Schaak, C. Vesprini, M. Pignini, *J. Med. Chem.* **2007**, *50*, 3964–3968.
- [27] A. E. Moormann, B. S. Pitzele, P. H. Jones, G. W. Gullikson, D. Albin, S. S. Yu, R. G. Bianchi, E. L. Sanguinetti, B. Rubin, M. Grebner, M. Monroy, P. Kellar, J. Casler, *J. Med. Chem.* **1990**, *33*, 614–626.

- [28] M. J. Bishop, K. A. Barvian, J. Berman, E. C. Bigham, D. T. Garrison, M. J. Gobel, S. J. Hodson, P. E. Irving, J. A. Liacos, F. Navas III, D. L. Saussy, Jr., J. D. Speake, *Bioorg. Med. Chem. Lett.* **2002**, *12*, 471–475.
- [29] L. Tottie, P. Baeckstrom, C. Moberg, J. Tegenfeldt, A. Heumann, *J. Org. Chem.* **1992**, *57*, 6579–6587.
- [30] K. Tsuna, N. Noguchi, M. Nakada, *Tetrahedron Lett.* **2011**, *52*, 7202–7205.
- [31] J.-H. Deng, H.-M. Tai, C.-C. Yang, *J. Chin. Chem. Soc.* **2000**, *47*, 327–341.
- [32] W. Quaglia, A. Piergentili, F. Del Bello, Y. Farande, M. Giannella, M. Pignini, G. Rifaiani, A. Carrieri, C. Amantini, R. Lucciarini, G. Santoni, E. Poggesi, A. Leonardi, *J. Med. Chem.* **2008**, *51*, 6359–6370.
- [33] V. N. Viswanadhan, A. K. Ghose, G. R. Revankar, R. K. Robins, *J. Chem. Inf. Comput. Sci.* **1989**, *29*, 163–172.
- [34] C. Wang, Y. Jiang, J. Ma, H. Wu, D. Wacker, V. Katritch, G. W. Han, W. Liu, X. P. Huang, E. Vardy, J. D. McCorvy, X. Gao, X. E. Zhou, K. Melcher, C. Zhang, F. Bai, H. Yang, L. Yang, H. Jiang, B. L. Roth, V. Cherezov, R. C. Stevens, H. E. Xu, *Science* **2013**, *340*, 610–614.
- [35] B. Y. Ho, A. Karschin, T. Branchek, N. Davidson, H. A. Lester, *FEBS Lett.* **1992**, *312*, 259–262.
- [36] J. Mialet, Y. Dahmoune, F. Lezoualc'h, I. Berque-Bestel, P. Eftekhari, J. Hoebeke, S. Sicsic, M. Langlois, R. Fischmeister, *Br. J. Pharmacol.* **2000**, *130*, 527–538.
- [37] W. Kuipers, R. Link, P. J. Standaar, A. R. Stoit, I. Van Wijngaarden, R. Leurs, A. P. IJzerman, *Mol. Pharmacol.* **1997**, *51*, 889–896.
- [38] B. L. Roth, M. Shoham, M. S. Choudhary, N. Khan, *Mol. Pharmacol.* **1997**, *52*, 259–266.
- [39] A. Carrieri, A. Piergentili, F. Del Bello, M. Giannella, M. Pignini, A. Leonardi, F. Fanelli, W. Quaglia, *Bioorg. Med. Chem.* **2010**, *18*, 7065–7077.
- [40] M. Bourin, M. C. Colombel, M. Maligne, J. Bradwejn, *J. Psychiatry Neurosci.* **1991**, *16*, 199–203.
- [41] P. Willner, *Psychopharmacology* **1984**, *83*, 1–16.
- [42] K. Ushijima, H. Sakaguchi, Y. Sato, H. To, S. Koyanagi, S. Higuchi, S. Ohdo, *J. Pharmacol. Exp. Ther.* **2005**, *315*, 764–770.
- [43] A. G. Sartim, F. S. Guimarães, S. R. Joca, *Behav. Brain Res.* **2016**, *303*, 218–227.
- [44] C. M. Tan, L. E. Limbird in *The Receptors: The Adrenergic Receptors in the 21st Century* (Ed.: D. Perez), Humana Press Inc., Totowa, NJ, **2006**, pp. 241–265.
- [45] Schrödinger Release 2015-3: Maestro, version 10.3, Schrödinger, LLC, New York, NY, **2015**.
- [46] A. Šali, T. L. Blundell, *J. Mol. Biol.* **1993**, *234*, 779–815.
- [47] R. A. Laskowski, M. W. MacArthur, D. S. Moss, J. M. Thornton, *J. Appl. Crystallogr.* **1993**, *26*, 283–291.
- [48] P. C. D. Hawkins, A. G. Skillman, A. Nicholls, *J. Med. Chem.* **2007**, *50*, 74–82.
- [49] G. M. Morris, D. S. Goodsell, R. S. Halliday, R. Huey, W. E. Hart, R. K. Belew, A. J. Olson, *J. Comput. Chem.* **1998**, *19*, 1639–1662.
- [50] G. M. Morris, R. Huey, W. Lindstrom, M. F. Sanner, R. K. Belew, D. S. Goodsell, A. Olson, *J. Comput. Chem.* **2009**, *30*, 2785–2791.
- [51] W. D. Cornell, P. Cieplak, C. I. Bayly, I. R. Gould, K. M. Merz, Jr., D. M. Ferguson, D. C. Spellmeyer, T. Fox, J. W. Caldwell, P. A. Kollman, *J. Am. Chem. Soc.* **1995**, *117*, 5179–5197.
- [52] K. J. Bowers, E. Chow, H. Xu, R. O. Dror, M. P. Eastwood, B. A. Gregersen, J. L. Klepeis, I. Kolossvary, M. A. Moraes, F. D. Sacerdoti, J. K. Salmon, Y. Shan, D. E. Shaw, “Scalable Algorithms for Molecular Dynamics Simulations on Commodity Clusters” in *Proceedings of the ACM/IEEE Conference on Supercomputing (SC06)*, Tampa, FL, **2006**, November 11–17.
- [53] Schrödinger Release 2015-3: Desmond Molecular Dynamics System, version 4.3, D. E. Shaw Research, New York, NY, **2015**. Maestro-Desmond Interoperability Tools, version 4.3, Schrödinger, New York, NY, **2015**.
- [54] C. Kilkenny, W. J. Browne, I. C. Cuthill, M. Emerson, D. G. Altman, *J. Pharmacol. Pharmacother.* **2010**, *1*, 94–99.
- [55] N. Collinson, G. R. Dawson, *Psychopharmacology* **1997**, *132*, 35–43.
- [56] A. Dias Elpo Zomkowski, A. Oscar Rosa, J. Lin, A. R. Santos, J. B. Calixto, A. Lúcia Severo Rodrigues, *Brain Res.* **2004**, *1023*, 253–263.
- [57] R. D. Porsolt, A. Bertin, M. Jalfre, *Arch. Int. Pharmacodyn. Ther.* **1977**, *229*, 327–336.

---

Received: July 25, 2016

Revised: August 30, 2016

Published online on September 30, 2016